OPTOELECTRONICS AND ADVANCED MATERIALS – RAPID COMMUNICATIONS Vol. 4, No. 5, May 2010, p. 759 - 763

Local observations of primary production in the Ross Sea: results of a lidar-calibrated satellite algorithm

R. FANTONI, L. FIORANI[a*], I. G. OKLADNIKOV[c], A. PALUCCI[a]
ENEA, UTAPRAD, Via Fermi 45, 00044 Frascati, Italy
[a]ENEA, UTAPRAD-DIM, Via Fermi 45, 00044 Frascati, Italy
[b]SCERT, IMCES, Akademicheskii Avenue 10/3, 634055 Tomsk, Russia

Comparison studies between satellite estimates and in situ measurements of primary production demonstrate that satellite chlorophyll-a bio-optical algorithms need regional calibrations, especially in the Southern Ocean. In this research, the data of the ENEA lidar fluorosensor collected during the 16th Italian Antarctic Oceanographic Campaign have been used to calibrate the chlorophyll-a algorithm of the Sea-viewing Wide Field-of-view Sensor in three hydrographic regions of the Ross Sea: Terra Nova Bay, Cape Adare zone and center of the Ross Gyre. The results show that non-regional calibrated chlorophyll-a algorithms could misestimate primary production up to 50% – 75%. Finally, the corrected values of primary production have been calculated monthly and yearly in each of the abovementioned hydrographic regions. The values are in agreement with those found by other authors and provide information on the spatio-temporal distribution of primary production.

(Received May 06, 2010; accepted May 20, 2010)

Keywords: Primary production, Lidar, Radiometers, Algorithms

1. Introduction

Mixing processes involving water masses of the Ross Sea result in the definition of oceanographic provinces [Budillon et al. 2003] where the development of endemic phytoplankton is favored [Boyd 2002]. Recent studies demonstrate that the lack of knowledge of the taxonomic composition and of the bio-optical properties of the dominant species in an oceanographic province may result in a significant misestimate of its chlorophyll-a (Chl-a) content [Alvain et al. 2004]. In particular, there is a growing convergence indicating that the Chl-a content of the Southern Ocean is underestimated by ocean color satellite radiometers [Arrigo et al. 1998], as in the case of the Sea-viewing Wide Field-of-view Sensor (SeaWiFS) [Hooker et al. 1992]. This explains the need of in situ measurements in the oceanographic provinces of the Ross Sea, as those carried out by the ENEA lidar fluorosensor (ELF) [Barbini et al. 2001], on board the Research Vessel Italica. Moreover, if one wants to take advantage of the global coverage provided by ocean color satellite radiometers, a careful attention should be paid in atmospheric corrections [Fiorani et al. 1998] and calibrations/validations [O'Reilly et al. 2000] involving in situ measurements. Usual match up analysis of satellite versus in situ Chl-a values relies in relatively few stations were seawater samples are analyzed by HPLC: for example, the Chl-a comparison between satellite retrievals and in situ data from the fourth SeaWiFS reprocessing is based on 262 match ups [McClain et al. 2004]. On the contrary, many lidar measurements can be compared with one satellite retrieval: ELF emits a laser pulse every 0.1 s and, as a result, acquires thousands of signals during the time taken by the ship to span a satellite pixel [Barbini et al. 2004]. Moreover, while a station cover only one point of a pixel, ELF data represent a wider zone because they are distributed along a track crossing the pixel. As far as primary productivity (PP) is concerned, taking into account that Chl-a is the main variable of the vertically generalized production models [Behrenfeld and Falkowski 1997], one should expect that the Chl-a algorithms for satellite sensors [O'Reilly et al. 1998] require a regional calibration [Barbini et al. 2003] for an accurate assessment of PP in those oceanographic provinces.

A PP calculation calibrated with ELF in the whole Ross Sea has already been described in a previous paper [Barbini et al. 2005] and the interested reader will find there details and references on satellite sensors, ELF, Chl-a algorithms and PP models: here we focus only on the calibration with ELF of that PP calculation in key regions of the Ross Sea.

2. Regional models of primary productivity

The hydrographic regions of Terra Nova Bay (TNB), Cape Adare zone (CA) and center of the Ross Gyre (RG) are among the most interesting of the Ross Sea [Budillon et al. 2003]:

- the TNB polynya is the area where the high salinity shelf water (HSSW) is generated by formation and removal of ice; it is strongly affected by ice melting and nutrient release from the Drygalsky Glacier (case II waters);
- the northward branch of HSSW mixes with the modified circumpolar deep water (MCDW) near CA and escapes in the northern continental shelf break;

- in RG nutrients are released into the upper ocean by water mixing processes, favoring the onset of intense phytoplankton blooms; RG is located in the Joides Basin, near the continental shelf break (case I waters).

The zones under study are defined as follows (Fig. 1):

- TNB: -74.5 S – -75.25 S, 163 W – 166 W (0°.75 × 3°),
- CA: -71.5 S – -73 S, 170 W – 175 W (1°.5 × 5°),
- RG: -73.5 S – -74.5 S, 173 W – 177 W (1° × 4°).

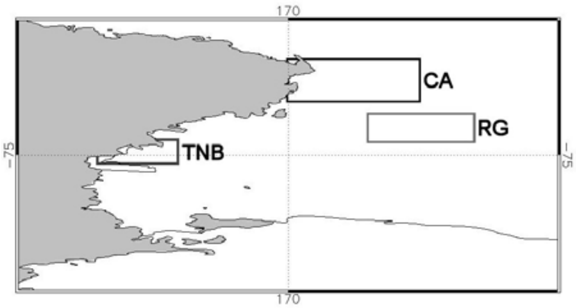

Fig. 1. Zones under study: Terra Nova Bay (TNB), Cape Adare (CA) and center of the Ross Gyre (RG).

Another interesting hydrographic region is the coastal belt from the Ross Island along the Ross Ice Shelf. It has not been included because the ELF-calibration does not significantly improve the SeaWiFS Chl-a bio-optical algorithm. Nevertheless, that large polynya area is a powerful supply for the Ross Sea PP.

The SeaWiFS Chl-a bio-optical algorithm has been calibrated in TNB, CA and RG with the ELF measurements of the 16th Italian Antarctic Oceanographic Campaign (January 5th 2001 – February 26th 2001). The procedure differs from that already described in a previous paper [Barbini et al. 2005] only for the calculation of the linear fit. The details of the statistical treatment can be found elsewhere [Fantoni et al. 2005].

Table 1. Results of the ELF calibration of the SeaWiFS Chl-a bio-optical algorithm in TNB, CA, RG and RSR.

Zone	Number of concurrent measurements	a_0	a_1
TNB	158	0.09	-3.1
CA	126	0.56	-2.3
RG	92	0.78	-2.7
RSR	1345	0.37	-1.4

The results of the ELF calibration of the SeaWiFS Chl-a bio-optical algorithm for TNB, CA and RG, as well as those obtained in a previous paper [Barbini et al. 2005] for the Ross Sea Region (RSR), are resumed in Table 1 and shown in Fig. 2. RSR has been defined as the area delimited by the coast and a line, straight in the cylindrical equidistant projection, from a point near Cape Adare (72° S, 170° E) to a point near Cape Colbeck (76° S, 158° W) [Barbini et al. 2005]. It has to be pointed out that RSR contains the highly productive Ross Ice Shelf polynya.

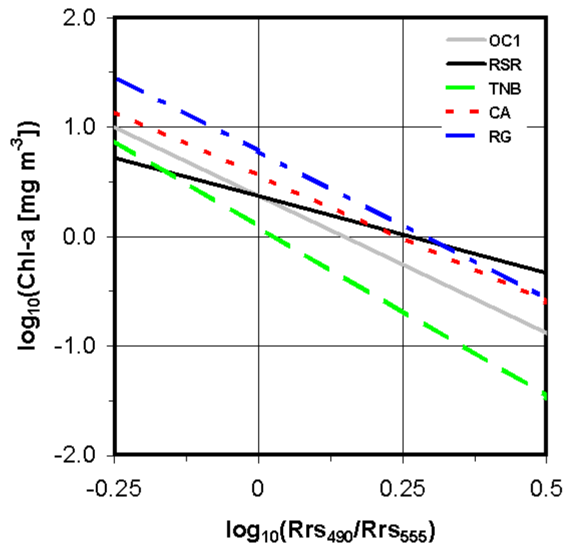

Fig. 2. Comparison among different SeaWiFS Chl-a bio-optical algorithms: OC1 (gray), ELF-calibrated during the 16th Italian Antarctic Oceanographic Campaign in RSR (black), TNB (green), CA (red) and RG (blue).

In the measurement range of the 16th Italian Antarctic Oceanographic Campaign ($-0.25 < \log_{10}(R_{490}/R_{555}) < 0.5$) our results indicate that:

- in TNB, standard OC1 [O'Reilly et al. 1998] overestimate Chl-a, especially at low concentrations (up to 75%),
- in CA, standard OC1 underestimate Chl-a, especially at low concentrations (up to 70%),
- in RG, standard OC1 underestimate Chl-a, especially at high concentrations (up to 50%).

As expected:

- the algorithm calibrated in CA and RG (mostly open sea and only open sea, respectively) is the closest to OC1 (calibrated typically with measurement stations in the open sea),
- the algorithm calibrated in RSR, a sort of average algorithm of the Ross Sea, lies almost in the midst of those calibrated in TNB, CA and RG.

The PP in TNB, CA and RG has been calculated with the D'-model, already described in a previous paper [Barbini et al. 2005]. The D'-model is a vertically generalized production model [Behrenfeld and Falkowski 1997] calibrated in Antarctic coastal waters [Dierssen et al. 2000] and corrected with the photosynthetically active radiation (PAR) measured by ELF during the 16th Italian Antarctic Oceanographic Campaign. PP is proportional to Chl-a in the D'-model and, as a consequence, the new PP values could differ from the standard data up to 50% – 75%.

The results are shown in Fig. 3. In the first part of the oceanographic campaign, few radiometer data are available on TNB, CA, and RG. The available measurements show a low productivity. From the 10th day, in TNB, and from the 17th and 18th day, in RG and CA, respectively, more radiometer data are available. While the PP of CA and RG is about one half of that of RSR, TNB is characterized by a high PP, showing values larger than in RSR (note the peak reaching nearly 2 gC m^{-2} d^{-1} in the 33rd day). Moreover, the PP decreases more slowly in TNB than in RSR.

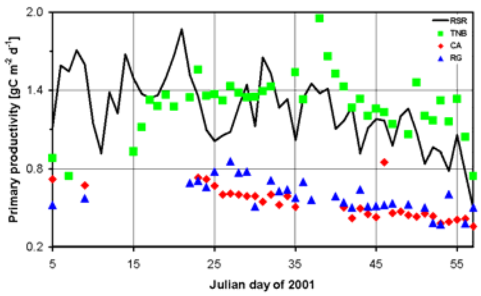

Fig. 3. PP calculated with the ELF-calibrated SeaWiFS Chl-a bio-optical algorithm in combination with the D'-model in RSR (black line), TNB (green squares), CA (red diamonds) and RG (blue triangles) coming from data collected during the 16th Italian Antarctic Oceanographic Campaign.

The ELF-calibrated SeaWiFS Chl-a bio-optical algorithm and the D'-model have been also used for a new estimate of the PP in TNB, CA and RG during the Austral summers from the launch of SeaWiFS, in 1997 (Fig. 4). Looking at Fig. 4, we can observe some interesting patterns.

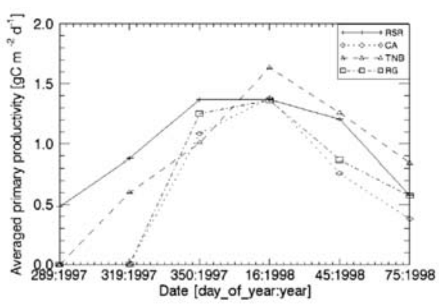

(a)

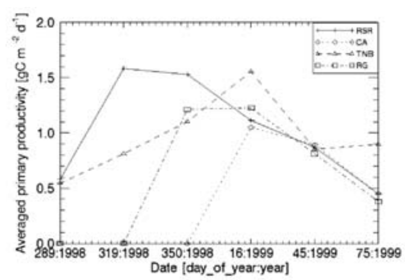

(b)

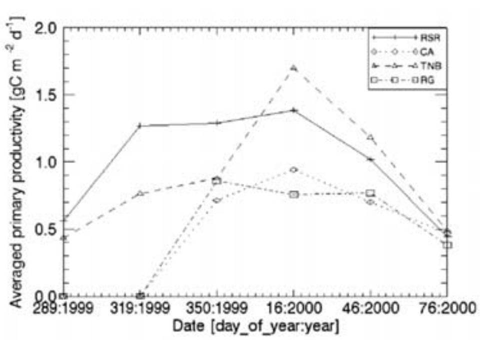

(c)

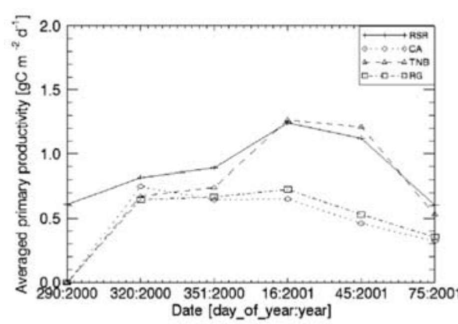

(d)

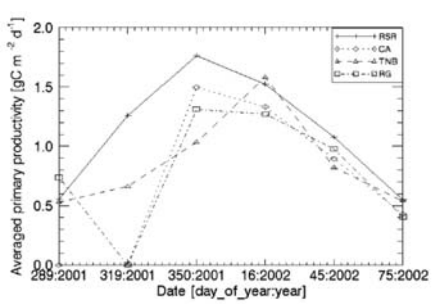

(e)

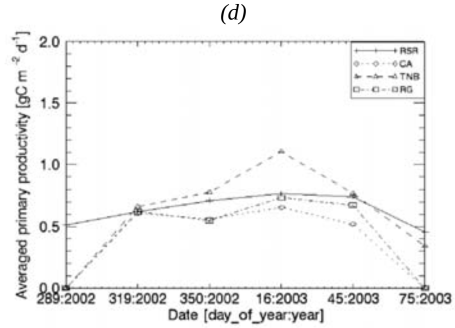

(f)

Fig. 4. Average PP calculated with the ELF-calibrated SeaWiFS Chl-a bio-optical algorithm in combination with the D'-model in RSR (crosses), TNB (triangles), CA (diamonds) and RG (squares).

Firstly, the PP curve in RSR is wider for all summers. It can be higher or lower than in TNB, CA and RG because it takes into account the contributions from hydrographic regions different from those specifically under study. The maximum can be reached before or after December. In particular, the marked early bloom development in Fig. 4 (b) and (c) can be ascribed to the Ross Ice Shelf polynya because it appears before the peak in TNB.

Secondly, TNB polynya results to be the second determining factor in PP because it strongly affects the overall behavior of RSR in summer. This effect is especially marked in January. The curves are compatible with two developing stages: earlier, in October, and later, in January, as already described in the literature [Lazzara et al. 2000]. The balance between the two phases depends on the season and is mainly driven by oceanographic forcings (wave motion, wind speed, sea tides and thermohaline currents) occurring in the two areas.

Thirdly, we can observe that, in general, the phytoplankton bloom in CA and RG is weaker, begins later and is close to the maximum already before January. In both areas HSSW, characterized by high nutrient concentration and low temperature, flows in deep layers along the continental slope. Differences in seasonal productivity are mainly due to phytoplankton transport under icebergs moving from the coastal to the offshore zone.

Eventually, looking at the sea ice concentration [Cavalieri et al. 2003], we can conclude that primary productivity is correlated with ice coverage, at least partially: the most and the least productive summers, 2001-2002 and 2002-2003, in that order, correspond to a small and a large ice coverage of the Ross Sea, respectively.

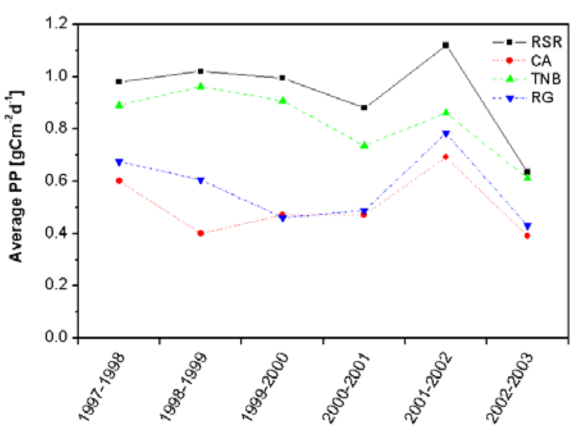

Fig. 5. Average PP calculated with the ELF-calibrated SeaWiFS Chl-a bio-optical algorithm in combination with the D'-model in RSR (black), TNB (green), CA (red) and RG (blue) from the Austral summer 1997-1998 to the Austral summer 2002-2003.

In order to observe yearly trends, the average primary productivity in the above mentioned summers have been evaluated (Fig. 5). It is confirmed that 2001-2002 and 2002-2003 are the most and the least productive periods in CA, RG and all the Ross Sea. Also in TNB 2002-2003 is the least productive period, but the maximum PP in TNB is reached in 1998-1999. This is not surprising because TNB is usually ice-free, and thus less sensitive to the ice coverage of the remaining part of the Ross Sea. In particular, it was so in all considered periods, except 2002-2003 [Cavalieri et al. 2003]. The average PP found in this study compares well with literature data [Arrigo et al. 1998].

3. Conclusions

The regional lidar calibration of a satellite PP model in three important hydrographic provinces of the Ross Sea have been described. The results of the present study show, from one hand, that the standard PP model should be reviewed, from the other hand, that the Chl-a algorithm has to be locally calibrated in each oceanographic province in order to provide accurate data: non-local models applied to standard surface Chl-a concentrations could misestimate PP in a hydrographic province up to 50% – 75%.

PP has been calculated monthly and yearly with the new models in each oceanographic region. The values compare well with those independently found by other authors and provide a mean to understand the phytoplankton dynamics both in each investigated region and in the whole Ross Sea, clarifying the role of each region in the overall PP during each season and from one year to another one. The deeper insight on the PP spatio-temporal distribution helps in recognizing the links between biogeochemical factors and algal blooms.

Acknowledgements

This work has been supported by PRNA–Oceanographic Sector–8.3 Project "ARES–active and passive remote sensing of the Southern Ocean for the monitoring of the biological parameters". The constant encouragement of R. Barbini and the important contribution of F. Colao are kindly acknowledged. The authors would like to thank the SeaWiFS Project (Code 970.2) and the Distributed Active Archive Center (Code 902) at the Goddard Space Flight Center, Greenbelt, MD 20771, for the production and distribution of these data, respectively. These activities are sponsored by NASA's Mission to Planet Earth Program.

References

[1] S. Alvain, C. Moulin, H. Loisel, Y. Dandonneau, E-proceedings of Ocean Optics XVII. ONR, Fremantle, Australia, CD-ROM, 2004.
[2] K. R. Arrigo, D. Worthen, A. Schnell, M. P. Lizotte, Journal of Geophysical Research C **103**, 15587 (1998).

[3] R. Barbini, F. Colao, L. De Dominicis, R. Fantoni, L. Fiorani, A. Palucci, E. S. Artamonov, International Journal of Remote Sensing **25**, 2095 (2004).
[4] R. Barbini, F. Colao, R. Fantoni, L. Fiorani, I. G. Okladnikov, A. Palucci, J. Optoelectron. Adv. Mater. **7**(2), 1091 (2005).
[5] R. Barbini, F. Colao, R. Fantoni, L. Fiorani, A. Palucci, J. Optoelectron. Adv. Mater. **3**(4), 817 (2001).
[6] R. Barbini, F. Colao, R. Fantoni, L. Fiorani, A. Palucci, International Journal of Remote Sensing **24**, 3205 (2003).
[7] M. J. Behrenfeld, P. G. Falkowski, Limnology and Oceanography **42**, 1479 (1997).
[8] P. W. Boyd, Journal of Phycology **38**, 844 (2002).
[9] G. Budillon, M. Pacciaroni, S. Cozzi, P. Rivaro, G. Catalano, C. Ianni, C. Cantoni, Antarctic Science **15**, 105 (2003).
[10] D. Cavalieri, P. Gloerson, J. Zwally, DMSP SSM/I Daily Polar Gridded Sea Ice Concentrations. NSIDC, Boulder, US, 2003.
[11] H. M. Dierssen, M. Vernet, R. C. Smith, Antarctic Science **12,** 20 (2000).
[12] R. Fantoni, L. Fiorani, A. Palucci, I. G. Okladnikov, Regional models for satellite measurements of primary productivity in the Southern Ocean. ENEA, Rome, Italy, 2005.
[13] L. Fiorani, S. Mattei, S. Vetrella, Proceedings of SPIE **3496,** 176 (1998).
[14] S. B. Hooker, W. E. Esaias, G. C. Feldman, W. W. Gregg, C. R. McClain, In: Hooker, S. B. and Firestone, E. R. (Eds.), SeaWiFS Technical Report Series. NASA, Greenbelt, US, **1**, 1992.
[15] L. Lazzara, V. Saggiomo, M. Innamorati, O. Mangoni, L. Massi, G. Mori, C. Nuccio, In: Faranda, F., Guglielmo, L. and Ianora, A. (Eds.), Ross Sea Ecology. Italiantartide Expeditions (1987-1995). Springer-Verlag, Berlin, Germany, 259, 2000.
[16] C. R. McClain, G. C. Feldman, S. B. Hooker, Deep-Sea Research **II**(51), 5 (2004).
[17] J. E. O'Reilly, S. Maritorena, B. G. Mitchell, D. A. Siegel, K. L. Carder, S. A. Garver, M. Kahru, C. McClain, Journal of Geophysical Research **C103**, 24937 (1998).
[18] J. E. O'Reilly, S. Maritorena, M. C. O'Brien, D. A. Siegel, D. Toole, D., Menzies, R. C. Smith, J. L. Mueller, B. Greg Mitchell, M. Kahru, F. P. Chavez, P. Strutton, G. F. Cota, S. B. Hooker, C. R. McClain, K. L. Carder, F. Müller-Karger, L. Harding, A. Magnuson, D. Phinney, G. F. Moore, J. Aiken, K. R. Arrigo, R. Letelier, M. Culver, In: Hooker, S. B. and Firestone, E. R. (Eds.), SeaWiFS Postlaunch Technical Report Series. NASA, Greenbelt, US, **11**, 2000.

* Corresponding author. luca.fiorani@enea.it